EFFECT OF ANKLE JOINT POSITION ON BIPED ROBOT WALKING BEHAVIOUR

Van-Tinh Nguyen[a], Ngoc-Linh Tao[b], Hiroshi Hasegawa[c]

[a], [b], [c]Graduate School of Engineering and Science
Shibaura Institute of Technology, Japan
[a]School of Mechanical Engineering
Hanoi University of Science and Technology, Vietnam

[a]nb16508@shibaura-it.ac.jp, [c] h-hase@shibaura-it.ac.jp

ABSTRACT
This paper addresses the effect of ankle joint position on the walking behavior of a biped robot. The mentioned foot structure consists of a tiptoe and a big toe inspired by the human foot which have a crucial role on moving stability. The study subject is a small robot called Kondo KHR-3HV, belonging to the Kondo Kagaku Company. Due to the small size of the robot and considering a reduction in energy consumption in toe mechanism, a passive joint using torsion spring was selected as a toe joint. The gait generation method, for finding the proper position of ankle joint, is used by varying the ankle joint position. There are two requirements of robot design: go straight and stay within setting conditions. The paper is implemented by two stages. First, the biped robot locomotion is considered by different stiffness coefficients to find out what is the proper stiffness coefficient. In the second stage, the simulation of all small biped robot models which have the different ankle joint position, can walk within setting conditions, is implemented. The results are compared to the human ankle joint trajectory in gait performance and frequency and are confirmed by dynamic simulation on Adams (MSC company, USA).

Keywords: biped robot, ankle joint position, walking behavior, big toe, torsion spring

1. INTRODUCTION
The human body has a complicated physical structure and implements difficult movements. During the past several decades, many researchers in the world have concentrated on the field of the biped robot inspired by the human body (Sakagami et al. 2002; Lohmeier et al. 2004; Ogura et al. 2006a; Ishida et al. 2004). The first aim of researches carried out in this field attempts to solve the following problem: "How can the robot walk naturally and stably?". This goal is motivated by several applications of the biped robot development such assistance, entertainment and medical issues. Hence, they have to move in a domestic environment and should have the same ability as humans to carry out stable walking.

In almost every previous studies, the feet of the biped robot have been designed with the rigid flat sole structure which cannot provide the best contact with the ground while in locomotion. Sometimes, it is a point contact at the corner of the sole as depicted in Figure 1, thus, the number of the contact point is reduced. Consequently, the support polygon area and the stability of the robot also decrease.

Furthermore, one of the characteristics of human walk is heel-contact and toe-off motion in steady walking. To implement adaptive walking, a foot is one of the most important regions of the human body in bipedal locomotion because it is the only region that has a direct physical interaction with the environment. The human foot has a complicated structure which consists of toes and several joints. On a human walking cycle, this structure makes the ground reaction force smoothly change in toe-off. Thus, it helps the contact between human foot and ground be smooth, having an important role in walking stability.

To overcome this challenge, from human foot inspiration, there have been some papers mentioned on the flexible foot structure for the biped robot. For instance, Yu Ogura et al. have proposed a new foot mechanism by implementing one passive joint for bending toe motion of Wabian-2R. However, in this study, the number of the robot's Degree of Freedom (DoF) is reduced due to the predetermination is complemented by waist rolling motion (Ogura et al. 2006b). Yamane and Trutoiu (2009) have investigated feet composed of curved surfaces at toe and heel and also a flat section for a simple planar biped robot. Sellaouti et al. (2006) have developed a new model of the humanoid robot HRP-2 with passive tiptoe joints to enhance its walking speed. Lohmeier et al. (2006) have designed the humanoid robot LOLA with an actively driven toe joints. However, the above-mentioned papers mainly focus on the humanoid robot whose parameters are similar to the human's ones. The human-size robots are very convenient for designing structure and integrating an actuator on the feet.

However, for a small bipedal robot, it is difficult to build a foot structure by limited parameters. Nerakae and Hasegawa (2014a) have presented the foot mechanism with big toe and tiptoe for a 10 DoFs small bipedal robot. The mentioned foot structure equips the robot with a good adaptation. It enables the foot to increase the contact points and improves the stability as described in Figure 2. Nevertheless, in the above-mentioned work, the trajectories of all the joints on both legs are generated by seven isolated gait functions which make a gait pattern generation become complicated. Simultaneously, the robot cannot walk naturally in comparison to the human motion. In addition, the torsion stiffness coefficients are only considered with two values and the ankle joint position is fixed based on the reference of the real robot. It is unreasonable because of the changed robot foot structure.

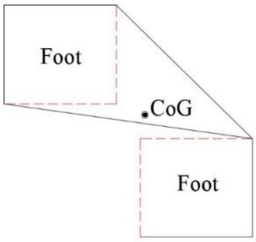

Figure 1: An example presenting the contact points, the support polygon and its center of gravity

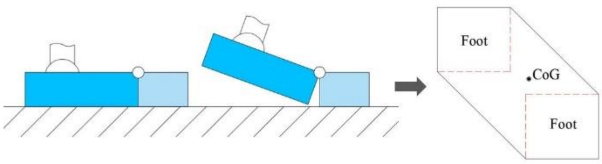

Figure 2: An adaptive foot structure

This study continues to develop a foot structure for a small robot proposed by Nerakae and Hasegawa (2014b). The paper implements to investigate the effect of two characteristics: spring stiffness and ankle joint position on robot walking behaviour. This is to aim to determine the consistent stiffness coefficient for toe joints when the robot performs its locomotion on flat ground. In the second stage, the simulation results of all small biped robot models when changing ankle joint position is compared with human walking behaviour to witness the effect of the changed ankle joint position on the robot walking behaviour and gait functions. It can be said that its walking style, in comparison to those of the other small biped robots, is more similar to that of humans.

This paper is organized in the following manner: A mechanical description of robot is presented in Section 2. The principle of gait pattern generation is in Section 3. Section 4 mentions the simulation procedure. Section 5 shows the results of the development of the robot by dynamic simulation on ADAMS. Finally, Section 6 includes some brief conclusions and future works.

2. EXPERIMENTAL ROBOT MODEL

2.1. Overview of structural design

In this study, the proposed model is built based on the KHR-3HV robot of the Kondo Kagaku Company which is the third generation of humanoid robots developed by this company. The KHR-3HV robot has the weight of 1.5kg, the height of 401.05mm and up to 22 DOFs with 17 actual servos and 5 dummy servos. However, in this work, only the robot's legs are focused on. Thus, the upper body joints are fixed and the lower body has 10 controlled joints for the legs as shown in Figure 3.

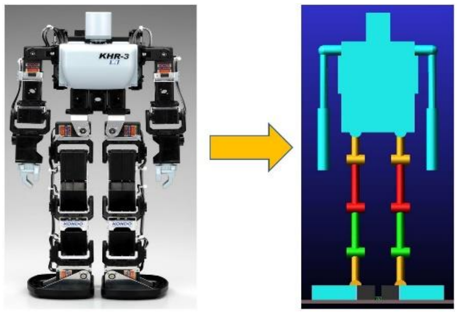

Figure 3: Real robot and experimental model

2.2. Foot mechanism

During locomotion, the human feet support area continuously varies on the sole of each foot as depicted in Figure 4. The black area is the position where supports force areas. Wherewith, LR is heel only in loading response, MSt is foot flat in mid stance, TSt is forefoot and toes is terminal stance, and PSw is medial forefoot in pre-swing. Perry and Burnfield (2010a) found that toe contact with ground is quite variable. The onset of toe involvement followed insolated forefoot support by 10% of the stance period. In this period, toe pressures differ markedly with the greatest pressure of the big toe. It ranged between 30% and 55% of that at the heel. Thus, the big toe has an important role in the human walking, especially during the toe-off period.

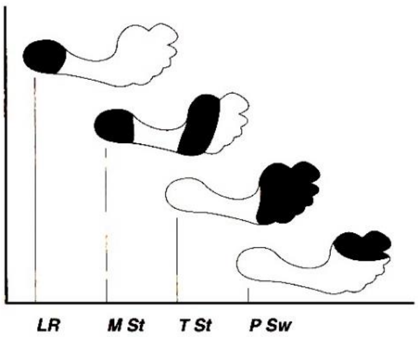

Figure 4. Sequence of foot support areas during stance (Perry and Burnfield 2010b)

By this idea, Nerakae and Hasegawa (2014c) have proposed the foot structure for enhancing the walking behavior of the biped robot as depicted in Figure 5. Their study exhibited that the big toe is a significant part to support and transfer weight from one foot to another foot.

However, in their paper, some parameters are predefined or referred to the real robot such as torsion stiffness coefficient and ankle joint position. Thus, this work is based on the assumption that those mentioned parameters have an effect on the walking behavior, walking distance and gait function. It is considered in a predefined range as described in Table 1 and Table 2.

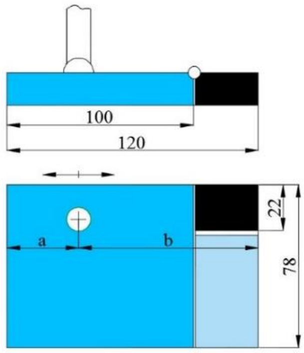

Figure 5. Robot foot structure

Table 1: Torsion spring stiffness coefficient

N_o	d(mm)	T(Kg.mm/210°)
M1	9.30	5.88
M2	9.37	7.60
M3	9.53	10.60
M4	11.71	13.71
M5	11.81	16.82
M6	11.81	17.40
M7	11.96	22.81
M8	14.12	27.19
M9	14.33	38.14
M10	14.45	45.28

Table 2: Ankle joint position

N_o	a(mm)	b(mm)	R=a/(a+b)
F1	80	40	0.67
F2	70	50	0.58
F3	60	60	0.50
F4	50	70	0.42
F5	40	80	0.33
F6	30	90	0.25
F7	20	100	0.17

3. GAIT FUNCTION

The joint angles are defined as described in Figure 6. The range of the angle is based on human motion data as Table 3.

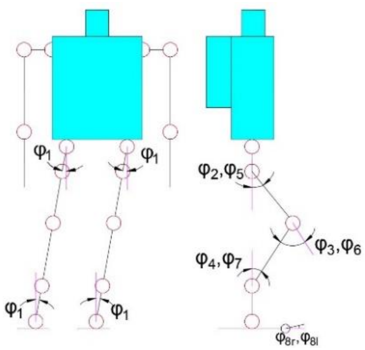

Figure 6. Robot linkage model

Based on the human walking pattern as depicted in Whittle (2007a), the paper supposes that the robot control data was generated by the gait function as a trigonometric function shown in Equation (1).

$$\varphi_i(t) = a_i + b_i.\cos(\omega t) + c_i.\sin(\omega t) + d_i.\cos(2\omega t) \qquad (1)$$

Table 3: The range of joint angle

Angle	View plane	Leg	Joint	Value
φ_1	Frontal	Both	Hip & ankle	-15° to 15°
φ_2	Sagittal	Right	Hip	-50° to 50°
φ_3	Sagittal	Right	Knee	0° to 60°
φ_4	Sagittal	Right	Ankle	-50° to 50°
φ_5	Sagittal	Left	Hip	-50° to 50°
φ_6	Sagittal	Left	Knee	0° to 60°
φ_7	Sagittal	Left	Ankle	-50° to 50°
φ_{8r}	Sagittal	Right	Proximal phalanx	0° to 30°
φ_{8l}	Sagittal	Left	Distal phalanx	0° to 30°

Where φ_i is the angle of i joint, a, b, c, d are coefficients, t is time, and ω is angular velocity. By changing a, b, c, d coefficients, the gait function will be created to allocate to each joint of the robot.

In this study, the bipedal robot is considered the locomotion on flat ground with the total time of 4.8 seconds. The robot is simulated in 3 cycles with a time period of 3.6 seconds, 1.2 left seconds are used for checking robot stability. One cycle is set up to 1.2 seconds. As a results, the angular velocity is calculated by Equation (2). In simulation, one step takes 0.02 second, the total number of step is 240. In the second cycle, the biped robot performs its motion the most natural, hence this cycle will be selected to show the waveform of the gait function as well as the robot walking behavior.

$$\omega = \frac{2\Pi}{1.2} = 5.236 \qquad (2)$$

Gait functions are assigned to all joints as shown in Equation (3-9).

$$\varphi_1 = \begin{cases} 0, \ t = 0 \text{ or } t \geq 3.6 \\ \pm 1.5, \ t = 0.3 \text{ and } t = 3.3 \\ \varphi_1(t), \ 0.3 < t < 3.3 \end{cases} \qquad (3)$$

$$\varphi_2 = \begin{cases} 0, \ t \leq 0.3 \text{ or } t \geq 3.6 \\ \varphi_2(t + 0.6), \ 0.3 < t < 3.3 \\ 15, \ t = 3.3 \end{cases} \qquad (4)$$

$$\varphi_3 = \begin{cases} 0, \ t \leq 0.3 \text{ or } t \geq 3.6 \\ \varphi_3(t + 0.6), \ 0.3 < t < 3.3 \\ 30, \ t = 3.3 \end{cases} \qquad (5)$$

$$\varphi_4 = \begin{cases} 0, \ t \leq 0.3 \text{ or } t \geq 3.6 \\ \varphi_4(t + 0.6), \ 0.3 < t < 3.3 \\ 15, \ t = 3.3 \end{cases} \qquad (6)$$

$$\varphi_5 = \begin{cases} 0, & t = 0 \text{ or } t \geq 3.3 \\ 15, & t = 0.3 \\ \varphi_2(t), & 0.3 < t < 3.3 \end{cases} \quad (7)$$

$$\varphi_6 = \begin{cases} 0, & t = 0 \text{ or } t \geq 3.3 \\ 30, & t = 0.3 \\ \varphi_3(t), & 0.3 < t < 3.3 \end{cases} \quad (8)$$

$$\varphi_7 = \begin{cases} 0, & t = 0 \text{ or } t \geq 3.3 \\ 15, & t = 0.3 \\ \varphi_4(t), & 0.3 < t < 3.3 \end{cases} \quad (9)$$

In toe mechanism, due to considering a reduction in energy consumption of the robot, the passive joint is selected as a toe joint. Consequently, φ_{8r} and φ_{8l} have a value in the range from 0° to 30°. Their values depend on the robot's geometric posture as well as an impact force when the robot performs its motion.

4. SIMULATION PROCEDURE

The concept of the optimization process is shown as in Figure 7. Z_f and X_f denote the distance from initial position to final position along z axis and x axis in the robot locomotion, respectively. R_f is the angle of rotation. Definition of optimal design is described as Equation (10 - 17).

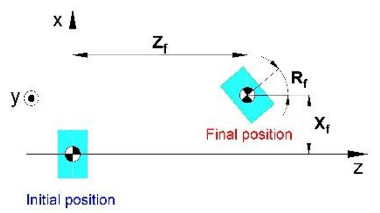

Figure 7. Overview of optimization

Design variables (DVs):

$$x = [a_i, b_i, c_i, d_i],\ i = 1\div4 \quad (10)$$

Constraint functions:

$$g_1(x) = 20 - |X_f| \geq 0 \quad (11)$$

$$g_2(x) = 5 - |R_f| \geq 0 \quad (12)$$

$$h_1(x) = 243.53 - Y_f = 0 \quad (13)$$

$$h_2(x) = N - 240 = 0 \quad (14)$$

Where Y_f is distance from Centre of Mass (CoM) to ground. N is a total simulation step.

Objective function:

$$f(x) = -Z_f \rightarrow \min \quad (15)$$

Penalty function:

$$P(x) = \sum_{i=1}^{2}\{\min[g_i(x), 0]\}^2 + \sum_{j=1}^{2}[h_j(x)]^2 \quad (16)$$

Modified objective function:

$$F(x) = -Z_f + \gamma.P \rightarrow \min \quad (17)$$

Where a_i, b_i, c_i, d_i (i=1, 2, 3, 4) are the coefficients of the gait function. There are four constraint functions. In Equation 11-12, X_f distance and R_f angle are constrained under ±20mm and ±5° to ensure that the biped robot can walk straight. In Equation 13, Y_f must be equal to 243.53mm to ensure the robot not to slip and fall down at the final framework. In Equation 14, N is equal to 240 to check the success of the simulation. In Equation 17, γ is a penalty coefficient set to 1000. Equation 11-14 will be also checked again when the simulation finishes.

5. SIMULATION RESULT

5.1. First experiment

The result is shown in Figure 8. As can be seen that all model can walk on flat ground. Side distance and angle of rotation in the simulation have a little difference when comparing with the calculation results on account of the approximating method. In consideration of walking straight and distance, model M7 with the stiffness coefficient of 22.81 Kg.mm/210° has the best performance. When the torsion stiffness increases, the long distance also go up, however, the side distance and angle of rotation have a same way. In contrast, this study plans to decrease the torsion stiffness, the long distance decreases. Thus, model 7 is selected to push the research further. The waveforms of the gait functions assigned to all joints are depicted in Figure 9. In comparison with the gait pattern of the human depicted in Whittle (2007b), as can be seen in Figure 9b and Figure 9c that the hip and the knee joint gait functions are similar to that of human beings. The difference of the ankle joint gait function is expected to occur as consequence of the physical structure dissimilarity with the humans' one.

5.2. Second experiment

The result of the second experiment is shown in Figure 10

The robot ankle joint trajectory of all experiments is shown in Figure 11, its data is collected in the second cycle since the biped robot performs the most natural and stable locomotion in this period. By comparison, human ankle joint trajectory is depicted in Figure 12. The subject in this study was a man. He was aged 47, 167 cm in height, and weighed 67 kg. This kinematic data for lower body while walking was measured using a Mac3D system (Motion Analysis Corporation). Data was recorded at a sampling rate of 200 Hz while the subject was walking.

As it can be seen, in general, the robot ankle joint trajectory has a frequency and a trend similar to the humans' one. From F1 to F7, the height of ankle joint change to adapt to the new ankle joint position. F7 position is near the robot's heel, and same as the human situation. However, the performance of this model is not so good. F4 and F5 position at the middle have the best performances which is the most comparable to human ankle joint trajectory, thus, these ankle joint positions are selected.

Waveform comparison of gait function assigned to all joints are depicted in Figure 13.

When the paper plans to change the ankle joint position from F1 to F7 as described in Table 2, the knee joint angle has gradually declined. The other joint angles are almost constant or change in small amount. Specially, the hip joint angle only has a small change at 0, 0.5, and 1 in a cycle. The ankle pitches joint angle changes at almost time. Figure 10 show that F5 model performs the best result, thus, this model should be selected for the next research in the future.

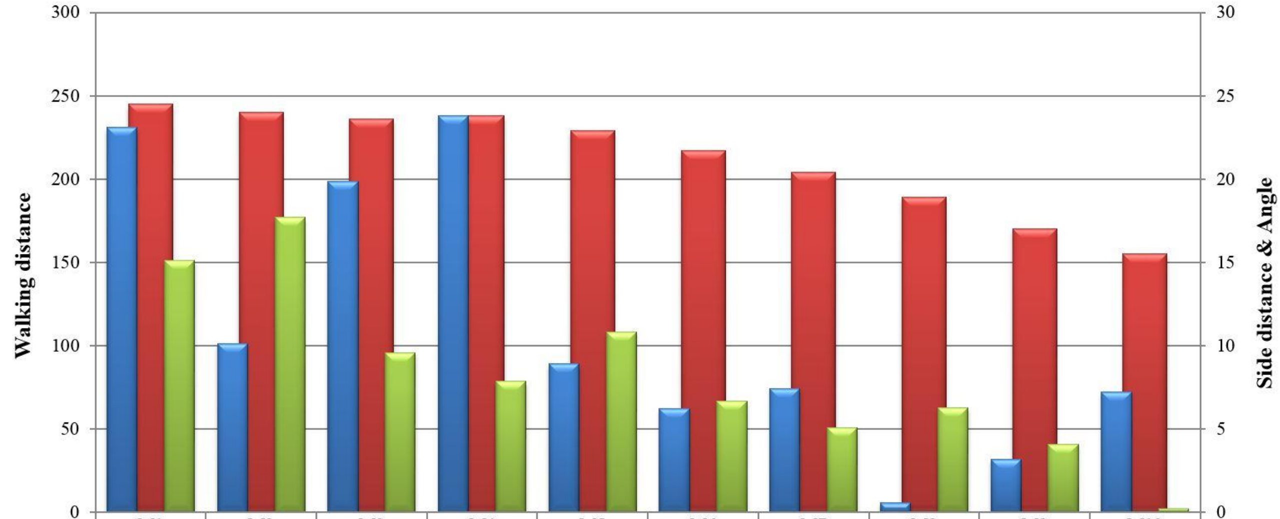

	M1	M2	M3	M4	M5	M6	M7	M8	M9	M10
Zd(mm)	245	240	236	238	229	217	204	189	170	155
|Xd|(mm)	23.10	10.14	19.87	23.81	8.92	6.20	7.43	0.58	3.18	7.24
|Rd|(deg)	15.12	17.69	9.59	7.87	10.84	6.68	5.10	6.28	4.08	0.21

Figure 8. Result of the first experiment

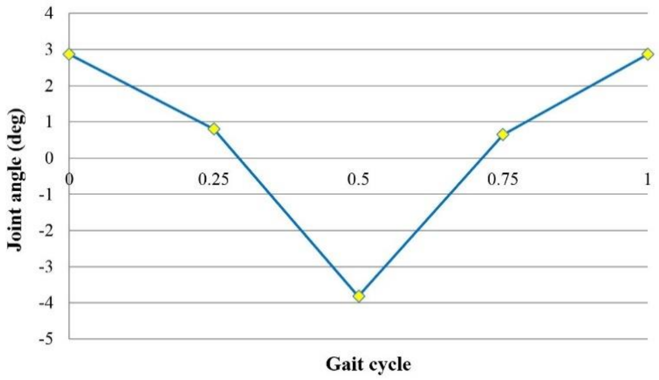

(9a) A cycle of gait function (hip and ankle roll joint angle)

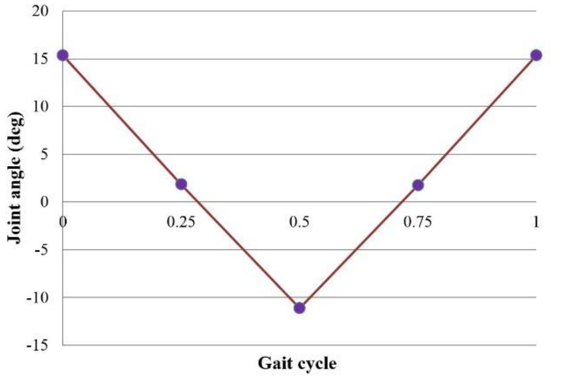

(9b) A cycle of gait function (hip pitch joint angle)

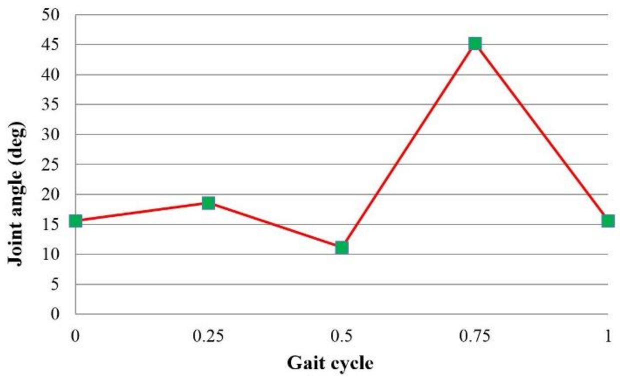

(9a) A cycle of gait function (knee pitch joint angle)

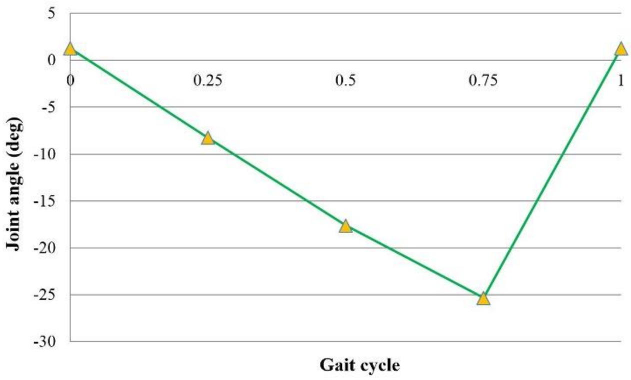

(9a) A cycle of gait function (ankle pitch joint angle)

Figure 9. Waveform of the gait function

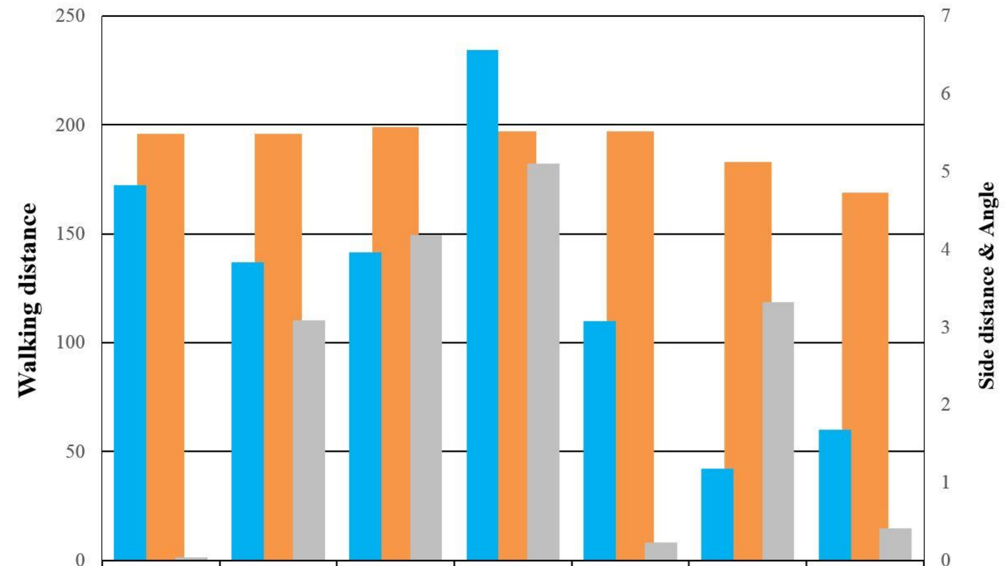

	F1	F2	F3	F4	F5	F6	F7
Zd(mm)	196	196	199	197	197	183	169
|Xd|(mm)	4.83	3.84	3.96	6.56	3.08	1.18	1.68
|Rd|(deg)	0.04	3.09	4.18	5.10	0.23	3.32	0.41

Figure 10. Result of the second experiment

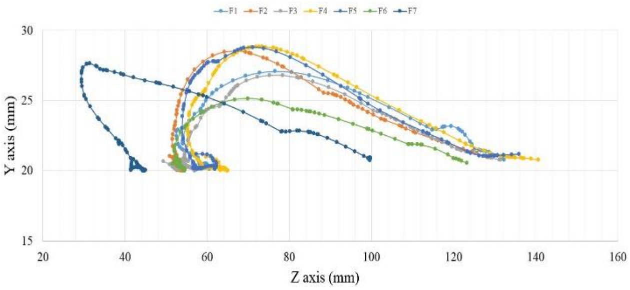

Figure 11. Robot ankle trajectory in a cycle

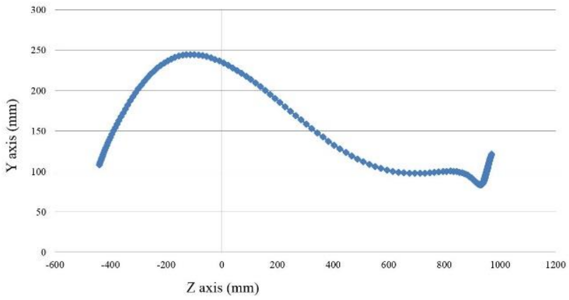

Figure 12. Human ankle trajectory in a cycle

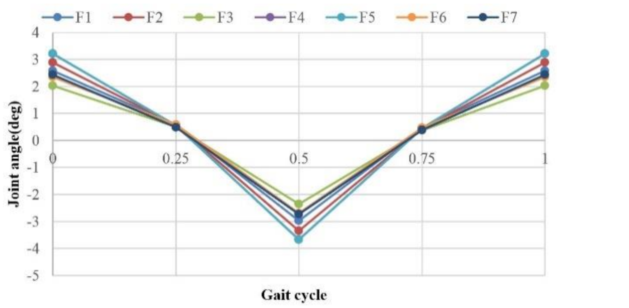

(13a) A cycle of gait function (hip and ankle roll joint angle)

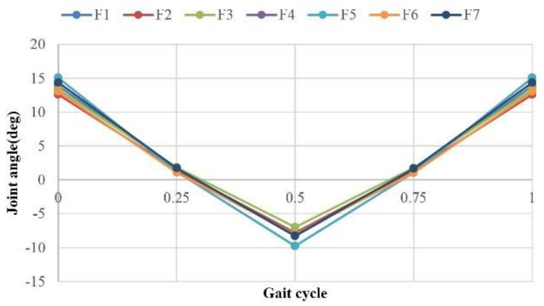

(13b) A cycle of gait function (hip pitch joint angle)

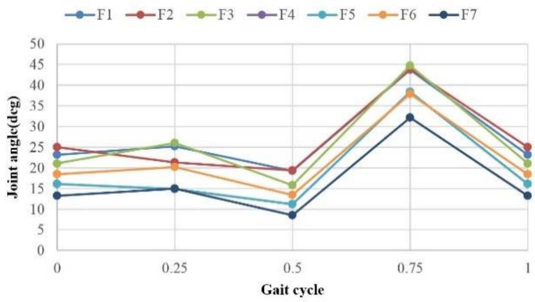

(13c) A cycle of gait function (knee pitch joint angle)

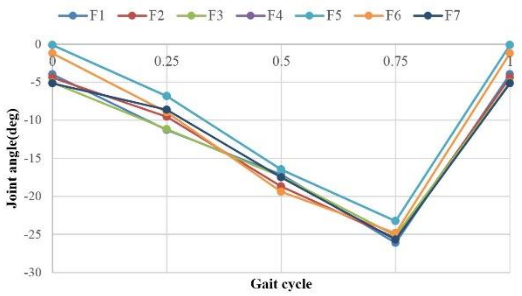

(13d) A cycle of gait function (ankle pitch joint angle)

Figure 13. Waveform of the gait function

6. CONCLUSIONS

The ankle joint position has the crucial effect on the walking behavior as well as the gait pattern of the biped robot. In this paper, the effect of two foot characteristics is considered. By the first experiment, the paper found out the most consistent spring stiffness coefficient for the proposed robot which is 22.81 Kg.mm/210^{o}. Through the second experiment, all models with changing ankle joint position can walk straight and within the constraint conditions. The gait functions are successfully generated by the approximated optimization method to each model. The robot ankle joint trajectory is compared with that of the human to find out the best position for the ankle joint.

For a future work, the study will plan to adjust the length of the toes to learn more and consider the locomotion of the robot on a rough ground.

REFERENCES

Sakagami Y., Watanabe R., Aoyama C., Matsunaga S., Higaki N., and Fujimura K., 2002. The intelligent ASIMO, system overview and integration. Proceedings of The IEEE/RSJ International Conference on Intelligent Robots and Systems, pp. 2478–2483, Switzerland.

Lohmeier S., Loffler K., Gienger M., Ulbrich H., and Pfeiffler F., 2004. Conputer system and control of biped "Johnnie". Proceedings of IEEE International Conference on Robotics and Automation, pp. 4222-4227, New Orleans, LA.

Ogura Y., Aikawa H., Shimomura K., Morishima A., Lim H. O., and Takanishi A., 2006. Development of a new humanoid robot WABIAN-2. Proceedings of IEEE International Conference on Robotics and Automation, pp. 830-835, Orlando, Florida.

Ishida T., 2004. Development of a Small Biped Entertainment Robot QRIO. Proceedings of the Fourth Symposium Micro-Nano mechatronics for Information-Based Society, pp. 23-28.

Yamane K., and Trutoiu L., 2009. Effect of Foot Shape on Locomotion of Active Biped Robots, a Study on Effect of Two-Arch Structure of Foot for Biped Robot. Proceeding of 9th IEEE-RAS International Conference on Humanoid Robot, pp. 2230-2236, Paris, France.

Sellaouti R., Stasse O., Kajita S., Yokoi K., and Kheddar A., 2006. Faster and smoother walking of Humanoid HRP-2 with passive toe joints. Proceedings of IEEE/RSJ International Conference on Intelligent Robots and Systems, pp. 4909-4914, Beijing, China.

Lohmeier S., Buschmann T., Ulbrich H., and Pfeiffer F., 2006. Modular joint design for performance enhanced humanoid robot LOLA. Proceedings of IEEE International Conference on Robotics and Automation, pp. 88-93, Florida, USA.

Nerakae K., and Hasegawa H., 2014. Big toe sizing design of small biped robot by using gait generation method. Applied Mechanics and Materials, 541-542 pp. 1079-86.

Perry J., and Burnfield J. M, 2010. Gait Analysis: Normal and Pathological Function, 2nd ed., Slack Incorporated, p. 82.

Whittle M. W., 2007. An Introduction to Gait Analysis. 4th ed., Oxford, p 59.

AUTHORS BIOGRAPHY

Van-Tinh Nguyen received the B.E. (2012) from Hanoi University of Science and Technology (HUST), Vietnam, and M.E. (2016) from Shibaura Institute of Technology (SIT), Japan. Besides, he works as a lecturer at School of Mechanical Engineering of HUST. Currently, he is pursuing Dr. Eng. degree in Functional Control Systems at SIT. His research interests include optimization system design, multi-body systems, humanoid robot, and evolutionary algorithm.

Ngoc-Linh Tao received his B.E. in 2010 at Hanoi University of Science and Technology, Vietnam and M.E. in 2013 from Taiwan University of Science and Technology, Taiwan. He is pursuing Dr. Eng. degree at the Department of Functional Control Systems, Graduate School of Engineering and Science, Shibaura Institute of Technology, Japan. His research interests include 3D computer vision and intelligent algorithms.

Hiroshi Hasegawa received his B.E. in 1992 and M.E. in 1994 from Shibaura Institute of Technology, Japan. He received Dr. Eng. In 1998 in mechanical engineering from Tokyo Institute of Technology, Japan. He has been working at Shibaura Institute of Technology, and currently is a Professor at the Department of Machinery and Control System, College of Systems Engineering and Science. He is a member of JSEE, JSME, ASME, JSCES, JSST and KES. His research interests include computer-aided exploration, creativity of design and systems engineering.